Evolutionary Intelligence (2025) 18:17
https://doi.org/10.1007/s12065-024-01001-x

RESEARCH PAPER

An efficient multilevel thresholding image segmentation through improved elephant herding optimization

Falguni Chakraborty[1] · **Provas Kumar Roy**[2]

Received: 26 July 2023 / Revised: 3 October 2024 / Accepted: 12 November 2024

Abstract

This paper proposed an improved version of recently developed swarm-based metaheuristic algorithm elephant herding optimization (EHO) called Improved Elephant Herding Optimization (IEHO). In this IEHO, the opposition-based learning (OBL) rule and chaos-embedded sequences are incorporated with each iterative stage of EHO to maintain the proper balance between the exploration and exploitation phase. It regulates the movement of the search agents and avoids premature convergence. The effectiveness of the proposed model is evaluated in terms of finding the optimal threshold value in Multilevel thresholding (MTH) of image segmentation which separates the different objects of the images. The methods such as the Kapur entropy, Otsu and masi entropy are used as the objective function in this problem to determine the optimal threshold. The proposed IEHO's performance is compared with the different variants of EHO, artificial bee colony (ABC) and artificial hummingbird algorithms (AHA). The simulation results regarding convergence speed, stability, and solution quality performance indicators, such as the structural similarity index (SSIM), feature similarity index (FSIM), and peak signal-to-noise ratio (PSNR) verify the viability of the above hybrid algorithm.

Keywords Chaos theory · Multilevel image segmentation · Elephant herding optimization · Oppositional chaotic elephant herding optimization

Abbreviations

EHO	Elephant herding optimization
IEHO	Improved elephant herding optimization
MTH	Mul-tilevel thresholding
AHA	Artificial hummingbird algorithms
SSIM	Structural similarity index
FSIM	Feature similarity index
PSNR	Peak signal-to-noise ratio
NFL	No free lunch
GA	Genetic algorithm
PSO	Particle swarm optimization
ABC	Artificial bee colony
DE	Differential evolution (DE)
BFO	Bacterial foraging optimization
ACO	Ant colony optimization
CSA	Cuckoo search algorithm
HBMO	Honey bee mating optimization
SSO	Social spider optimization
FP	Flower pollination
BAT	Bat algorithm
FDO	Fitness-dependent optimizer
ANA	Ant nesting algorithm
LPB	Larner performance based behavior
CDDO	Child drawing development optimization
OBL	Opposition-based learning
EA	Evolutionary algorithms
EWOA	Enhanced whale optimization algorithm
GWO	Grey wolf optimizer
OEHO	Oppositional elephant herding optimization
CEHO	Chaos-based elephant herding optimization
SA	Simulated annealing
FA	Firefly algorithm
MSE	Mean squared error
RGB	Red green blue
CBL	Chaostic based learning

✉ Falguni Chakraborty
falguni.durgapur@gmail.com

[1] Dr. B. C. Roy Engineering College, Durgapur, West Bengal, India

[2] Kalyani Government Engineering College, Kalyani, West Bengal, India

Published online: 30 November 2024

1 Introduction

1.1 Background

Multilevel image thresholding is a method of separating an image into different non-overlapping regions. These techniques work as the pre-processing step for image analysis, and nowadays, they are used to aid diagnosis in medical imaging, automate locomotion for robotics and self-driving cars, and identify objects of interest in satellite images. In case of complex medical images, MTH has become the most preferred choice among researchers as it can affect all spatial domains of the images, which helps to reducing the effect of noise. Among the various advances accessible in the literature for image segmentation, thresholding-based segmentation approaches based on pixel value intensity have gained massive popularity due to their simplicity and accuracy. Threshold-based segmentation is a non-parametric approach to image segmentation in which a set of optimal thresholds is determined using optimization methods. The objective functions like Masi's entropy [29], Otsu's between class variance [22] and, Kapur's entropy method [17] are commonly utilized strategies for image thresholding. Hence, thresholding-based segmentation's primary challenge is to select the best sets of thresholds that maximize the thresholding procedure. In most cases, traditional optimization algorithms become inefficient in solving real-world problems because they fail to search for the best set of optimized threshold values. Nature-inspired meta-heuristic optimization algorithms are thought recently to be a promising solution in this regard.

1.2 Objectives and significance

In recent years, various swarm-based meta-heuristic algorithms have been reported in the literature to find the global optimization of various non-linear, non-convex, and non-differentiable optimization issues across a continuous search space. Swarm-based meta-heuristic algorithms are designed according to social animals' collective and clever behavior, such as ants, birds, fish, wolves, etc. have proved their potentiality to unravel different real-life troubles in the various areas of science and engineering.

Exploration and exploitation are the two leading factors of any meta-heuristic optimization algorithm. Proper balancing between these two factors leads to achieving global optima. Therefore, any optimization algorithm's main challenge is to preserve a reasonable adjustment between these two aspects. But most of the meta-heuristic techniques use the stochastic property to explore its search space, which causes weak convergence, and it stuck into local optima.

Therefore, developing and improving meta-heuristic algorithms is continuously needed to solve different types of optimization problems. Besides this, according to the No Free Lunch (NFL) theory [39], a single meta-heuristic algorithm may not produce a better result for all kinds of optimization. This fact motivates the researchers to developed or update the existing algorithms. Keeping this in mind, in this study, we modify the EHO to make strides in the performance of the basic EHO within the areas of multilevel image thresholding.

1.3 Literature review

A swarm-based meta-heuristic optimization technique has become very useful in achieving this target. During the last few years, several such optimization techniques and their improved version have been reported in the literature for image segmentation. Example of few of the meta-heuristic algorithm are Genetic Algorithm (GA) [43], Biogeography Based Optimization (BBO) [30], Particle Swarm Optimization (PSO) [44], Artificial Bee colony (ABC) [3], Differential Evolution (DE) [32], Bacterial Foraging Optimization (BFO) [26], Ant Colony Optimization (ACO) [16], Cuckoo Search (CS) [7], Honey Bee Mating Optimization (HBMO) [15], Social Spider Optimization (SSO) and Flower Pollination (FP) [33], BAT Algorithm [41] etc. Fitness-Dependent Optimizer (FDO) [21], Ant Nesting Algorithm (ANA) [13], Learner Performance Based behavior algorithm (LPB) [8], Child Drawing Development Optimization (CDDO) [2]

In the literature, the OBL strategy has been integrated with many meta-heuristic algorithms to avoid sub-optimal issues, which causes premature con-vergence. It is mathematically proved that the inverse appraises of a solution are closer to the global solution than the arbitrary ones [35]. Hence, many authors have incorporated the concept of OBL with several evolutionary algorithms (EA) such as particle swarm optimization [46], artificial bee colony (ABC) [42], krill herd algorithm [31], differential evolution [24], etc. to avoid the local optima in searching the best optimal values.

Besides the OBL technique, chaotic-based optimization has also been used to prevent the algorithm from sticking at suboptimal points in exploring the search space comprehensively. Recently, the thought of employing chaotic orbits rather than a random number in the algorithm has become an active research area to bargain with the issue of premature convergence of meta-heuristic optimization. Examples of such chaos-based optimization are differential evolution algorithm [25], Darwinian particle swarm optimization [28], particle swarm optimization algorithm [11], firefly algorithm [10], bat algorithm [9], and cuckoo search algorithm [37].

In recent past various work has been reported in literature of multilevel segmentation. Sharma et al. (2022) [27] used hybrid Genetic Algorithm and Particle Swarm Optimization (GA-PSO) to detect brain cancers by multilevel segmentation of brain MRI data. Kim and colleagues (2023) [18] utilized the Firefly Algorithm to segment retinal images and identify diabetic retinopathy. In a subsequent investigation, Gupta et al. [12] proposed an enhanced whale optimization algorithm (EWOA) for the segmentation of lung CT images to identify lung cancer. Salima Ouadfel et al. [33] have used two recent nature-inspired meta-heuristics algorithms named SSO and FP algorithm for multilevel image thresholding. Pare [23] proposed modified fuzzy entropy as the segmentation method with the Levy flight firefly algorithm for thresholding of color images. In [6], authors have focused on color image segmentation using a different optimization technique. Khairuzzamanet al. [1] have used grey wolf optimizer (GWO) for image segmentation. In [14], the author proposes an altered firefly algorithm based on multilevel thresholding for color image segmentation. Aziz et al. [5] have utilized the whale optimization algorithm and moth-flame optimization for multilevel image thresholding.

1.4 Novelty and contributions

In this study, we have coordinated both the chaotic and opposition-based learning with the basic EHO to explore the better performance of the EHO. Combining these two strategies would help the EHO algorithm preserve the correct adjustment between exploration and exploitation. This proposed algorithm is evaluated to find the best suitable thresholds for image segmentation of some standard images using Masi's entropy, Otsu's between-class variance and Kapur's entropy method as the objective function. Also, we evaluated the algorithm performance statistically and checked the quality of the images using some quality metrics.

The following are the highlighted contributions of this work:

- An efficient OBL and chaotic-based EHO called IEHO to improve the performance of the basic EHO.
- Evolution of the effectiveness of the proposed algorithms for determining the optimal threshold in multilevel image thresholding for some standard images.
- An extensive comparative study among the different variants of EHO and other algorithms
- valuate the quality metrics such as FSIM, SSIM, and PSNR for verifying the quality of the images.
- The robustness of the proposed algorithm is proven in the present study by accessing the statistical analysis.

1.5 Structure of the paper

The remaining portion of the paper is structured as follows. The mathematical model of the image segmentation problem with the different image segmentation techniques is discussed in Sect. 2. Section 3 presents some recently proposed meta-heuristic optimization algorithms used for image segmentation. The proposed algorithm is described in Sect. 4. The Results, along with discussions, are presented in Sect. 5. Finally, we conclude in Sect. 6.

2 Mathematical model of the problem

Image segmentation problem is mathematically represented as:

$$\begin{aligned} R_{G_1} &\leftarrow R \text{ if } 0 \le R < TH_1 \\ R_{G_2} &\leftarrow R \text{ if } TH_1 \le R < TH_2 \\ R_{G_{n-1}} &\leftarrow R \text{ if } TH_{n-1} \le R < TH_n \\ R_{G_n} &\leftarrow R \text{ if } TH_n \le R < L-1 \end{aligned} \tag{1}$$

where $TH_1 < TH_2 < ..... < TH_{n-1} < TH_n$ are the thresholds values which divided the image into $R_{G_1}, R_{G_2}, ..., R_{G_n}$ regions.. The optimized threshold values TH_1,TH_2..., TH_n can be obtained by maximizing the following objective function

$$(TH_1^*, TH_2^*, ..., TH_n^*) = argmax(f(TH_1, TH_2, ..., TH_n)) \tag{2}$$

In the image segmentation problem, the optimized threshold values used for segmenting the images can be achieved by optimizing an objective function $f(.)$. In the proposed research work, two popular segmentation methods, namely Otsu's between class variance [22] and Kapur's [17] method are chosen. Moreover, one of the high performance-based segmentation methods namely, Masi's [29] entropy is used as the objective function.

The additive or non-additive properties are the two characteristics of images. Most entropy-based segmentation methods deal with the image's additive or non-additive properties. But masi entropy deals with both additive and non-additive properties. As a result, these methods produce better segmentation than the other objective functions. The details of the above objective functions are as follows:

2.1 Objective function

2.1.1 Kapur's objective function

Kapur's entropy is one of the well-known objective functions [17] used for computing the optimized thresholds for

image segmentation. Kapur's objective function (in terms of entropy) for dividing an image into $n+1$ different regions using n number thresholds is defined as follows:

$$f(t) = H_0 + H_1 + H_2 + ... + H_n \tag{3}$$

where $t = [t_1.t_2, t_3, ..., t_n]$

$$\begin{cases} H_0 = -\sum_{i=0}^{t_1-1} \frac{p_i}{\omega_0} ln \frac{p_i}{\omega_0} \\ H_1 = -\sum_{i=t_1}^{t_2-1} \frac{p_i}{\omega_1} ln \frac{p_i}{\omega_1} \\ H_2 = -\sum_{i=t_j}^{t_{j+1}-1} \frac{p_i}{\omega_2} ln \frac{p_i}{\omega_2} \\ H_n = -\sum_{i=t_{n-1}}^{L-1} \frac{p_i}{\omega_{n-1}} ln \frac{p_i}{\omega_{n-1}} \end{cases} \tag{4}$$

$H_0, H_1, ..., H_n$, are the Kapur's entropy for segmented region. The set of optimum thresholds (t^*) using Kapur's entropy is obtained by maximizing the following function:

$$t^* = [t_1^*, t_2^*, t_3^*, ..., t_n^*] = argmax(f(t)), \tag{5}$$

2.1.2 Masi's objective function

Masi's entropy of j^{th} segmented region of an image is computed by

$$M_j = \frac{1}{1-r} log\left[1 - (1-r)\sum_{i=t_j}^{L}\left(\frac{p_i}{\omega_j}\right) log\left(\frac{p_i}{\omega_j}\right)\right] \tag{6}$$

For $n+1$ regions and n thresholds, $0 \le j \le n$, and r is the entropic parameter which is set to 0.8. For segmenting n non-overlapping regions the Masi's objective function ($f(t)$) is defined as follows:

$$f(t) = M_0 + M_1 + M_2 + ... + M_n \tag{7}$$

where $t_1 < t_2 < t_3 ..... < t_n$ and the optimal thresholds (t^*) are calculated by optimizing the Masi's entropy as below:

$$t^* = [t_1^*, t_2^*, t_3^*, ..., t_n^*] = argmax(f(t)), \tag{8}$$

2.1.3 Otsu's objective function

Apart from these entropy-based objective functions, Otsu's between-class variance is another popular objective function for image thresholding. For n number of thresholds, the Otsu's objective function is given by,

$$f(t) = \sum_{i=0}^{n} \sigma_i \tag{9}$$

$$\begin{aligned} \sigma_0 &= \omega_0(\mu_0 - \mu_T)^2 \,,\ \sigma_1 = \omega_1(\mu_1 - \mu_T)^2 \\ \sigma_j &= \omega_j(\mu_j - \mu_T)^2 \,,\ \sigma_n = \omega_n(\mu_n - \mu_T)^2 \end{aligned} \tag{10}$$

where μ_T is the mean intensity of the whole image. The cumulative probability of each region can be calculated as:

$$\mu_0 = \sum_{i=0}^{t_1-1} \frac{ip_i}{\omega_i} \,,\ \mu_1 = \sum_{i=t_1}^{t_2-1} \frac{ip_i}{\omega_i} \,,\ \mu_j = \sum_{i=t_j}^{t_{j+1}-1} \frac{ip_i}{\omega_i} \,,\ \mu_n = \sum_{i=t_n}^{L-1} \frac{ip_i}{\omega_i} \tag{11}$$

The set of optimal thresholds (t^*) can be obtained by maximizing the objective function of the Eqn.(12)

$$t^* = [t_1^*, t_2^*, t_3^*, ..., t_n^*] = argmax(f(t)) \tag{12}$$

3 Improved elephant herding optimization (IEHO)

3.1 Elephant herding optimization (EHO)

Elephant herding optimization (EHO) is a newly developed meta-heuristic algorithm proposed by Wang et al. [36]. The herding behavior of the elephant in nature is mathematically modeled in two phases: clan updating operator and separating operator with the following assumption.

1. The elephant group comprises a fixed number of clans, and matriarch is the head of each clan.
2. Male elephants like to live alone, and they leave the group while developing.

3.1.1 Clan updating operator

In this phase, since the matriarch is the leader of each clan, other clan individuals overhaul their position by the impact factor of the matriarch by the following equation.

$$x_{new,c_i,j} = x_{c_i,j} + \alpha \times (x_{best,c_i} - x_{c_i,j}) \times r \tag{13}$$

Where $x_{best,ci}$ represents the matriarch of the clan c_i and $x_{new,ci,j}$ is the newly updated position of the j^{th} elephant of the clan c_i; matriarch influence factor is decided by the control parameter $\alpha \in [0, 1]$, and $r \in [0, 1]$, which follows the uniform distribution.

However, as the best elephant of the clan cannot be updated by the above equation, it is overhauled by the following equation.

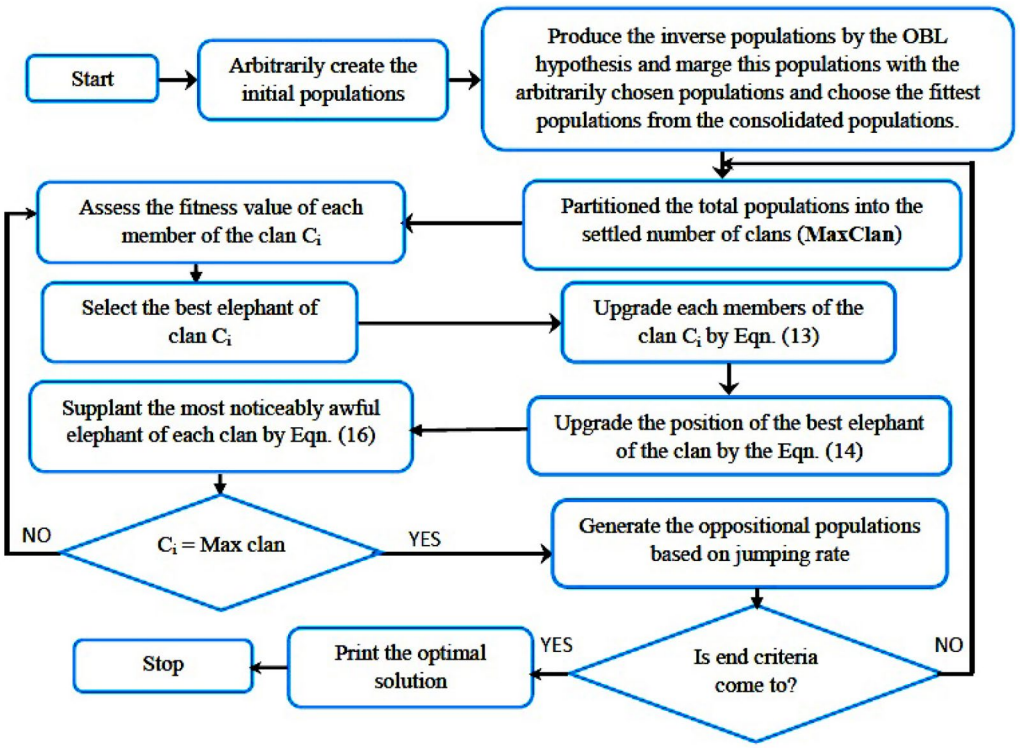

Fig. 1 Flowchart of OEHO

$$x_{new,c_i,j} = \beta \times x_{center,c_i} \tag{14}$$

The influence factor of $x_{center,ci}$ on $x_{new,ci,j}$ is decided by the control parameter $\beta \in [0, 1]$. The $x_{center,ci}$ of the clan c_i is calculated as follows.

$$x_{center,c_i,d} = \frac{1}{n_{c_i}} \times \sum_{n_{c_i}}^{j=1} x_{c_i} d \tag{15}$$

where n_{c_i} is the sum of elephants of each clan of the $d^t h$ dimension where $1 \leq d \leq D$, here D is dimension of the clan.

Table 1 List of chaotic maps

S.no	Neme	Chaotic map
1	LOGISTIC	$X_{n+i} = \lambda x_n(1 - x_n) \quad for \quad 0 < \lambda \leq 4$
2	TENT	$X_{n+i} = \begin{cases} \mu x_n & if \quad 0 < x_n \leq 0.5 \\ \mu(1 - x_n)x_n & if \quad 0.5 < x_n \leq 1 \end{cases} \mu = 1.25$
3	CHEBYSHEV	$X_{n+i} = cos(kcos^{-}1x_n)$
4	GAUSSIAN	$X_{n+i} = \begin{cases} 0 & x_n = 0 \\ \frac{1}{x_n} mod 1 & x_n \geq 0 \end{cases}$
5	SINE	$X_{n+i} = \frac{a}{4} sin(\pi x_i) \quad 0 < a \leq 4$
6	ITERATIVE	$X_{i+i} = \frac{a}{4} sin(\frac{a\pi}{x_i}) a \in [0, 1] \quad x \in [0, 1]$
7	SINUSOIDAL	$X_{i+i} = ax^2 sin(\pi x_i) \quad a = 2.3, x \in [0, 1]$
8	SINGER	$X_{i+i} = \mu(7.86x_i - 23.31x_i^2 + 28.75x_i^3 - 13.30287x_i^4) \quad where \quad \mu = 1.07$
9	CIRCLE	$Z_{n+i} = mod(x_i + b - \frac{a}{2\pi} sin(2\pi x_k, 1)$
10	CUBIC	$Z_{n+i} = \lambda x_n(1 - x_n^2) \quad for \quad 0 < \lambda \leq 4$

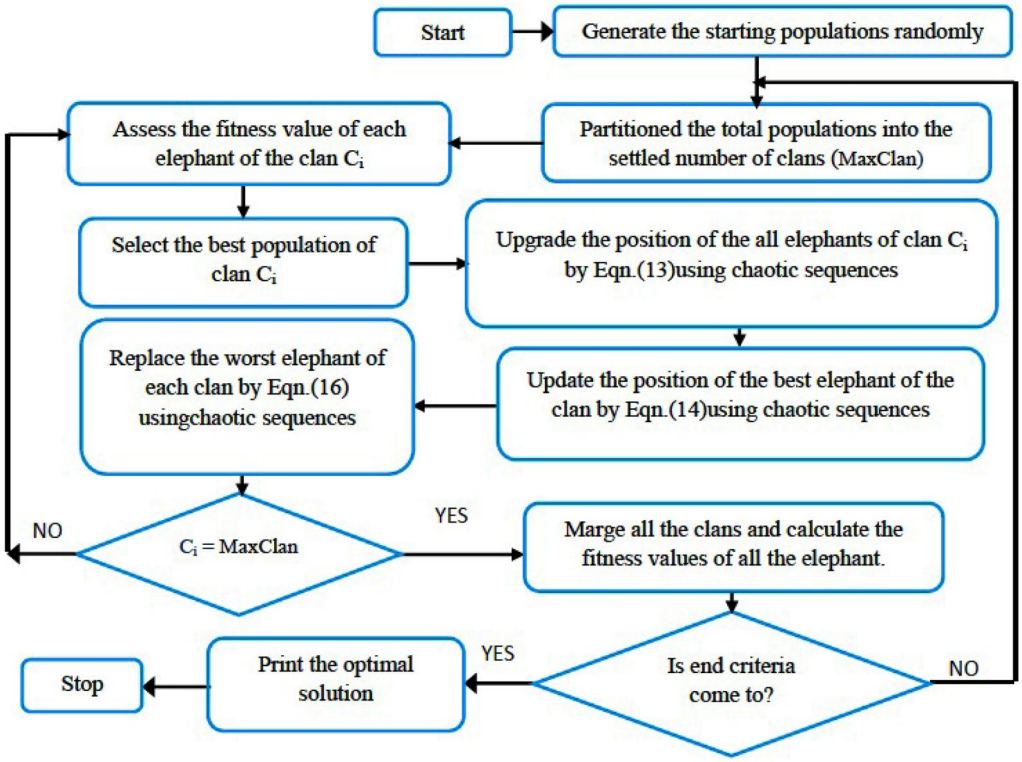

Fig. 2 Flowchart of CEHO

3.1.2 Separating operator

Male elephants in elephant group take off their clans when they reach adulthood. This herding behaviour is mathematically modeled as a separating operator. In each era, the most noticeably awful elephant (Minimum fitness value) of each clan changed their position by the following equation.

$$x_{wrost,c_i} = x_{min} + (x_{max} - x_{min}) \times r \tag{16}$$

where x_{worst,c_i} represents the most noticeably awful elephant of the clan c_i of elephant group; search space boundary is defined in between x_{max} and x_{min} and $r \in [0, 1]$ is arbitrary chosen from a group of uniformly distributed numbers.

3.2 Opposition based learning (OBL)

Generally, the starting population of evolutionary algorithms is arbitrarily characterized within the search space, and after that, it is overhauled in each consequent iteration and reaches the ideal solution. The convergence speed is relatively connected to the starting populations of the solutions. Therefore, closer to the starting assumption, less time is required to converge. Thus, to improve the initial solution, Tizhoosh [34] has proposed opposition-based learning (OBL) by concurrently assessing the current and contrary populations and selecting the fitter one as the introductory solution. In the probability theory, 50% of the time, a guess is an advance from the ideal solution than the inverse estimation. In this IEHO, the OBL strategy is incorporated in two ways: firstly, it is used to generate the initial population for quick convergence, and secondly, at the end of each iteration of the basic EHO based on the jumping probability, this OBL concept is used to dodge the ideal local solution.

Definitions of some useful term associated with OBL is given below.

3.2.1 Opposite number and opposite point

Opposite number ($\bar{x}$) of a real number is calculated as $\bar{x} = a + b - x$, where $x \in [a, b]$ similarly the opposite point of $X(x_1, x_2, \ldots, x_D)$ in D-dimensional space $\overline{X}(x_1, x_2, \ldots, x_D)$ is defined as

$$\bar{x} = a_i + b_i - x_i \quad \text{where} \quad X_i \in [a_i, b_i] \tag{17}$$

3.2.2 Opposition based optimization

Let in D-dimensional problem $\overline{X}(x_1, x_2, \ldots, x_D)$ be the opposite point of $X(x_1, x_2, \ldots, x_D)$, $f(X)$ and $f(\overline{X})$ are fitness values of current population and opposite population, respectively.

In maximization problem, if $(\overline{X}) \geq f(X)$, then X point is replaced by the $\overline{X}$.

3.2.3 Opposition based generation by jumping probability

The same method may be followed to improve the solution in each iteration depending on the jumping rate J_r. The jumping rate is a control parameter defined by the user to jump or skip opposite population creation at a certain generation to save the computation time.

Three different jumping rate or jumping probability have been defined as per literature [35] to explore the tuning ability of the proposed algorithm are defined as follows:

$$\begin{cases} J_r^{avg} = (J_r^{max} + J_r^{min})/2 \\ J_r^1 = (J_r^{max} - J_r^{min}) * ((NFC_{max} - NFC)/NFC_{max}) \\ J_r^2 = (J_r^{max} - J_r^{min}) * ((NFC_{max} - NFC)/NFC_{max}) - (J_r^{max} - J_r^{min}) \end{cases} \tag{18}$$

where maximum (J_r^{max}) and minimum (J_r^{min}) limits of J_r are 0 and 0.6, respectively. NFC_{max} is the maximum number of function calls, NFC is the number of function calls at the current iteration.

3.2.4 Opposition based EHO (OEHO)

The concept of OBL is utilized in basic EHO to enhance its performance [30]. The application of OBL helps generate a better starting population for quicker convergence on one side, and it helps the algorithm come out from local optima on the other side. The detailed flowchart of the oppositionalEHO (OEHO) is shown in Fig. 1.

3.3 Chaostic based learning (CBL)

Chaos is a branch of mathematics utilized to engender arbitrariness by the basic deterministic framework. It is exceptionally touchy to its starting condition. The astronomically immense number of chaotic sequences with diverse chaotic orbits can only be incited by transmuting the initial condition. The uncertainty, ergodicity, and stochastic property [40] of chaotic systems help produce the non-repetitive set of random numbers, which can help cover all the possible states in the search domain, confirming the visit to each stage a single time. It improves the stochasticity of the heuristic search process and avails in eluding local optimality [4].

This non-repetitive property of chaotic sequences motivates the researchers to use the chaotic sequence in the meta-heuristic algorithms to improve global optimization performance. In different real-life problems, various chaotic maps are successfully used to generate globally accepted solutions. Some widely used chaotic functions are collected from the literature [20] and shown in Table 1.

We have chosen 0.7 within the limiting range of values from 0 to 1 as the starting point. Among all maps, the robust performance of the Tent map makes it suitable for this problem domain. Hence, for this problem, Tent maps are used as the chaotic sequence generator, which replaces the stochastic nature of the EHO algorithm in each stage.

3.3.1 Chaos-based EHO (CEHO)

In this study, we have incorporated these chaotic phenomena with the basic EHO to expedite the convergence speed of the basic EHO. The detailed outlines of Chaotic EHO (CEHO) is shown in Fig. 2

3.4 Improved EHO (IEHO)

In IEHO, the initial populations are generated through the OBL, which helps to start with a better population that accelerates the search for global optima and also it helps to come out from local optima. The CBL concept is incorporated in clan updating operator and separating operator phases of the basic EHO. It replaces the stochastic nature of the variable with the chaotic sequence, which helps to search for better solutions by increasing the problem's search space.

The updated clan updating operator and separating operator of basic EHO are as follows:

3.4.1 Clan updating operator in IEHO

j^{th} elephant of clan c_i is updated as,

$$x_{new,c_{i,j}} = x_{c_{i,j}} + r_1 \times (x_{best,c_i} - x_{c_{i,j}}) \times r_2 \tag{19}$$

$$x_{new,c_{i,j}} = r_3 \times x_{center,c_i} \tag{20}$$

where r_1,r_2 and r_3 are the chaotic sequences and are generated by the Tent map with the different initial values

3.4.2 Separating operator in IEHO

In IEHO, the separating operation is done by using the following equation

$$x_{wrost,c_i} = x_{min} + (x_{max} - x_{min}) \times r_4 \tag{21}$$

Where the values of r_i are generated by using the Tent chaotic map with the different initial values. Besides, we apply the opposition based learning with chaotic EHO to get it out of sticking at local optima.

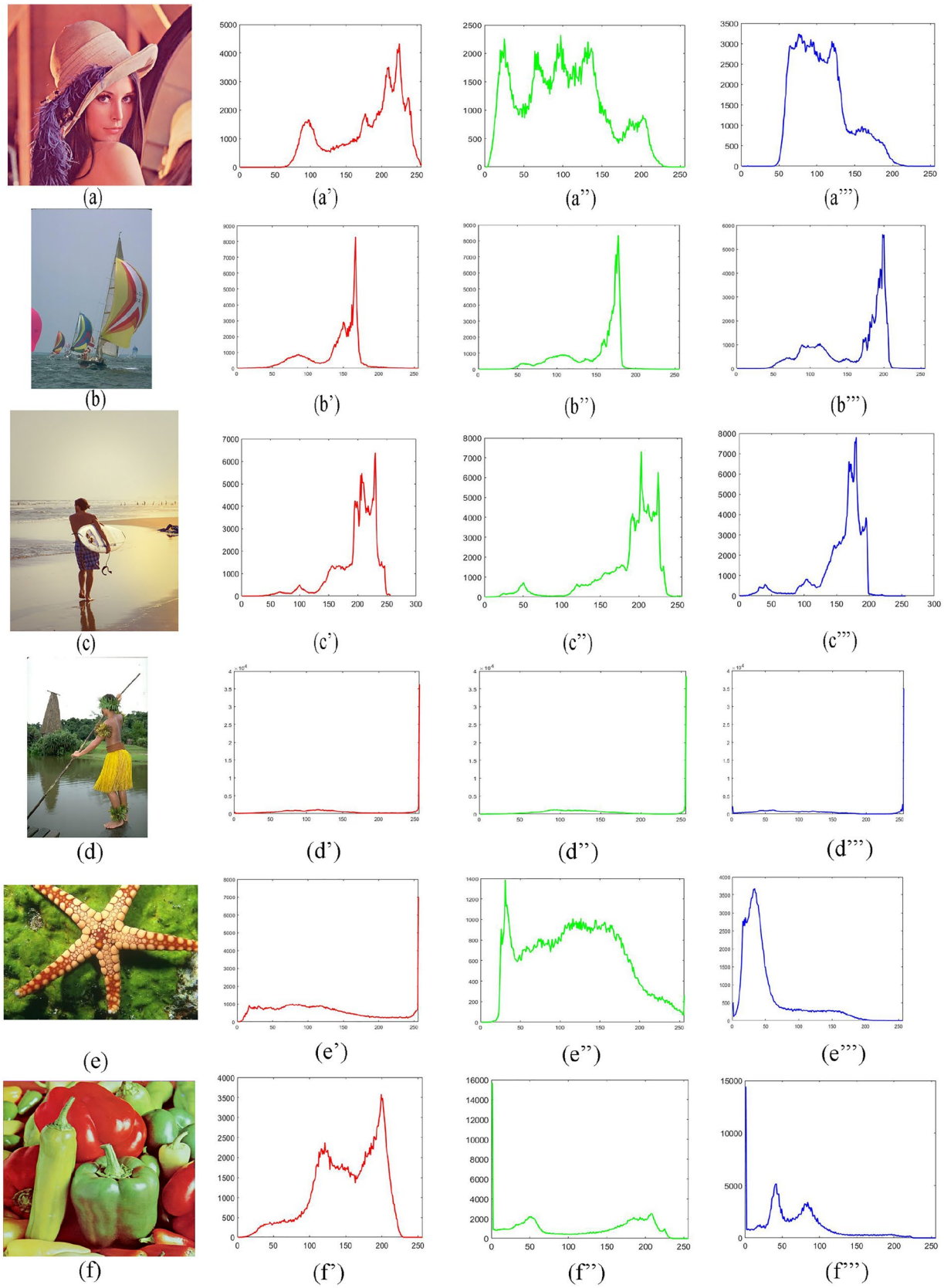

Fig. 3 List of test images along with its histogram of red, green and, blue band in RGB color space

Table 2 Parameters used for EHO, ABC, AHA algorithms

Algorithms	Parameter	Value
EHO	Number of nests	30
	No. of iterations	100
	Matriarch influence parameter (α)	0.9
	Influence factor of clan canter (β)	0.25
ABC	Swam size	30
	No. of iterations	100
	Lower bound and upper bound	1,256
	Value of ϕ	[0,1]
AHA	Population size (P)	30
	No. of iterations	100
	Migration coefficient	2*P

4 IEHO in multilevel image thresholding

The following are the steps for implementing IEHO algorithm in multilevel image thresholding.

- **Initialize ecosystem** :
  - Population size
  - Number of thresholds to calculate
  - Set the generation limit (Max_{Gen})
- **Select the starting population by concepts of OBL theory**.
- Evaluate fitness value of all the population of the ecosystem for selected color band of RGB color space.
- **Repeat**
- Choose the best organism (maximum fitness value)..
  - **Clan update operator Phase**.

    Each member of the clan are adjusted through Eqn.(19) except the finest elephant.
    Upgrade the position of the most excellent elephant by the Eqn.(20).
    Determine fitness value for new reformed elephant.
  - **End**
  - **Separating operator phase**.
  - Update the position of the most exceedingly bad member of each clan by the Eqn. (21).
  - **End**
- Determine fitness for altered elephants
- Merge all the clans to generate the population again.
- Alter the population according to OBL theory, when the jumping rate is $J_r \leq 0.35$
- **Until (Max_Gen)**

5 Experimental setup

The essence of the proposed IEHO-based multilevel image thresholding has been verified on a set of images with different intensity distributions collected from the benchmark database of Berkeley University. Images with their histogram are shown in Fig. 3. Experiments are carried out on a workstation with a PC with a 2.30 GHz CPU, 8.00 GB RAM, and a Windows 10 environment. MATLAB 2022b is used for writing and executing the codes.

As the performance of any population based optimization approach largely depends on its input parameters, they should be properly selected. To find its optimal input parameters, it is initially tested on "red band of the boat image" with different combination of input parameters. Table 3 shows average fitness value and computational time for twenty-five independent trials with different combinations of input parameters. It is found that the optimal settings of the input parameters *i.e*. Jumping probability, population size, iterations of IEHO for the red band of the boat image are found to be 0.4, 30 and 100 respectively. The increase of population size and iteration will unnecessarily increase the computation time without improving its fitness value. Therefore, throughout the experiment, the present authors fixed the population size to 30, and the halting condition with 100 iterations for all the algorithms to achieve an impartial assessment. The remaining parameters of all the algorithms are taken from the literature and are also shown in Table 2

5.1 Performance analysis

The proposed algorithm is applied separately for each image to find 5, 6, and 7 levels of thresholding. In this study the Otsu, Kapur's, and Masi's entropy-based segmentation technique are used as the objective function that are maximized with the proposed algorithms. The result accuracy and efficiency is validated by compared against chaotic and oppositional based EHO and two recently developed algorithms ABC, AHA. For the color images, the optimum threshold value is calculated separately for each red, green, and blues band for RGB color space. The optimum threshold values together with the maximum objective function values of the red, green, and blue bands of different segmentation methods are shown in Tables 5, 6 and 7. From the above table, It is established that the maximum calculated fitness values

Table 3 Optimal parameter selection for IEHO

Iteration	J_r	Fitness value	Computation time(sec)	Iteration	J_r	Fitness value	Computation time(sec)	Iteration	J_r	Fitness value	Computation time(sec)	Iteration	J_r	Fitness value	Computation time(sec)
Population =30															
50	0.6	26.1840	15.42	50	0.5	26.1840	15.31	50	0.4	26.1840	15.21	50	0.3	26.1840	15.31
75	0.6	26.1843	15.33	75	0.5	26.1843	15.32	75	0.4	26.1843	15.13	75	0.3	26.1840	15.23
100	0.6	26.1843	16.28	100	0.5	26.1865	16.39	100	0.4	26.2010	16.38	100	0.3	26.1843	16.48
125	0.6	26.1843	17.31	125	0.5	26.1865	17.41	125	0.4	26.2010	17.31	125	0.3	26.1843	17.42
150	0.6	26.1843	17.43	150	0.5	26.1865	17.43	150	0.4	26.2010	17.13	150	0.3	26.1843	17.53
175	0.6	26.1843	18.59	175	0.5	26.1865	17.47	175	0.4	26.2010	18.09	175	0.3	26.1843	18.18
Population =40															
50	0.6	26.1840	15.42	50	0.5	26.1843	15.42	50	0.4	26.1843	15.41	50	0.3	26.1843	15.41
75	0.6	26.1843	15.43	75	0.5	26.1843	15.44	75	0.4	26.1843	15.44	75	0.3	26.1843	15.16
100	0.6	26.2010	16.46	100	0.5	26.2010	16.45	100	0.4	26.2010	16.13	100	0.3	26.2010	16.46
125	0.6	26.2010	17.42	125	0.5	26.2010	17.41	125	0.4	26.2010	16.45	125	0.3	26.2010	17.45
150	0.6	26.2010	17.45	150	0.5	26.2010	17.46	150	0.4	26.2010	17.47	150	0.3	26.2010	17.46
175	0.6	26.2010	18.51	175	0.5	26.2010	18.5	175	0.4	26.2010	18.5	175	0.3	26.2010	18.52
Population =50															
50	0.6	26.1843	15.12	50	0.5	26.1843	15.0	50	0.4	26.1840	15.11	50	0.3	26.1840	15.50
75	0.6	26.1843	15.03	75	0.5	26.1843	15.04	75	0.4	26.1843	15.13	75	0.3	26.1843	15.14
100	0.6	26.2010	16.06	100	0.5	26.2010	16.25	100	0.4	26.2010	15.06	100	0.3	26.2010	16.15
125	0.6	26.2010	17.18	125	0.5	26.2010	17.14	125	0.4	26.2010	16.12	125	0.3	26.2010	17.12
150	0.6	26.2010	17.21	150	0.5	26.2010	17.4	150	0.4	26.2010	17.29	150	0.3	26.2010	17.12
175	0.6	26.2010	18.32	175	0.5	26.2010	18.22	175	0.4	26.2010	18.13	175	0.3	26.2010	18.14

for the Otsu, Kapur and Masi's objective function obtained through the proposed IEHO secure the 1st position among all the algorithms.

Segmented images of the proposed algorithm and the other chaotic and oppositional combination of EHO and others algorithms are shown in Figs. 4, 5, and 6. Images are reconstructed using the optimized red, green, and blue band of the RGB color space. The red band is optimized using Kapur's segmentation method, and the green and the blue band are optimized by Otsu's and Masi's entropy-based segmentation methods.

5.1.1 Evaluation metrics for segmented images

Peak signal-to-noise ratio (PSNR), structural similarity index metric (SSIM) [45] and feature similarity index metric (FSIM) [19] are the three quality matrices utilized in this study to measures the quality of the segmented images.

Peak signal-to-noise ratio (PSNR):

PSNR is used to measure the similarity of original and segmented images. It calculates the root mean square error (RMSE) of each pixel to find the difference of quality of original $I(i, j)$ and segmented $S(i, j)$ images. The PSNR can be defined as follows,

$$PSNR = 10Log_{10}\left(\frac{255^2}{RMSE}\right) \tag{22}$$

$$RMSE = \frac{\sum_i^M \sum_{j=1}^N |I(i,j) - S(i,j)|}{M * N} \tag{23}$$

The higher value of PSNR indicates better segmentation, which reflects a more effective segmentation process.

Structural similarity index metric (SSIM):

The SSIM [45], is another metric used to measure the internal structures between original (X) and segmented image (Y). It considers luminance, contrast, and structure to evaluate the image quality. Higher the value of SSIM shows the better internal similarity between the original and segmented images which indicates better segmentation SSIM and it is defined as under:

$$SSIM(x, y) = \frac{(2\mu_x\mu_y + c_1)(\sigma_{xy} + c_2)}{(\mu_x^2 + \mu_y^2 + c_1)(\sigma_x^2 + \sigma_y^2 + c_2)} \tag{24}$$

where μ_x and μ_y are mean intensities of original and segmented image; σ_x and σ_y are the standard deviations (SD) of the original and segmented image; σ_{xy} is the co-variance of original and segmented image. c_1 and c_2 are two constants, where c_1 and c_2 are taken as 0.01 and 0.03, respectively.

Feature similarity index metric (FSIM):

FSIM [19] is used to find feature similarity of two images $f_1(X)$ and $f_2(X)$ and is defined by:

$$FSIM = \frac{\sum_{X_\varepsilon \Omega} S_L(X) PC_m(X)}{\sum_{X_\varepsilon \Omega PC_m(X)}} \tag{25}$$

Table 4 Statistical analysis of the proposed algorithm using Wilcoxon rank sum test using Otsu's method as objective function

Image	K	IEHO vs. CEHO		IEHO vs. OEHO		IEHO vs. EHO		IEHO vs. ABC		IEHO vs. AHA	
		p	h	p	h	p	h	p	h	p	h
BOAT	5	>0.05#	0	>0.05 #	0	<0.05*	1	<0.05*	1	<0.05*	1
	6	<0.05*	1	<0.05*	1	>0.05#	0	<0.05*	1	>0.05*	0
	7	<0.05*	1	<0.05*	1	<0.05*	1	>0.05#	0	<0.05*	1
STARFISH	5	<0.05*	1	>0.05#	0	<0.05*	1	<0.05*	1	<0.05*	1
	6	<0.05*	1	<0.05*	1	<0.05*	1	>0.05#	0	>0.05*	0
	7	<0.05*	1	<0.05*	1	<0.05*	1	<0.05*	1	<0.05*	1
FISHING	5	>0.05#	0	<0.05*	1	>0.05 #	0	<0.05*	1	<0.05*	1
	6	<0.05*	1	<0.05*	1	<0.05*	1	<0.05*	1	>0.05*	0
	7	<0.05*	1	<0.05*	1	<0.05*	1	<0.05*	1	<0.05*	1
LENA	5	<0.05*	1	<0.05*	1	>0.05#	0	<0.05*	1	<0.05*	1
	6	<0.05*	1	<0.05*	1	<0.05*	1	<0.05*	1	<0.05*	1
	7	<0.05*	1	<0.05*	1	<0.05*	1	>0.05#	0	>0.05*	0
MAN	5	>0.05#	0	>0.05#	0	<0.05*	1	<0.05*	1	<0.05*	1
	6	<0.05*	1	<0.05*	1	>0.05#	0	<0.05*	1	>0.05*	0
	7	<0.05*	1	<0.05*	1	<0.05*	1	<0.05*	1	<0.05*	1
PEPPERS	5	<0.05*	1	>0.05#	0	<0.05*	1	<0.05*	1	<0.05*	1
	6	<0.05*	1	<0.05*	1	>0.05#	0	<0.05*	1	<0.05*	1
	7	<0.05*	1	<0.05*	1	<0.05*	1	<0.05*	1	>0.05*	0

Table 5 Fitness value along with the threshold values of different algorithms for red band of using Kapur's entropy as objective function

Image	K	IEHO	CEHO	OEHO	EHO	ABC	AHA	IEHO	CEHO	OEHO	EHO	ABC	AHA
BOAT	5	**21.1737**	21.1731	21.1731	21.1731	21.1731	21.1731	46 93 133 178 212	46 92 133 178 212	46 92 133 178 212	46 92 133 178 212	46 92 133 178 212	46 92 133 178 212
	6	**23.7985**	23.7947	23.7958	23.7958	23.7964	23.7958	38 67 100 133 178 212	38 67 101 134 178 212	42 70 101 134 178 212	42 70 101 134 178 212	41 67 101 134 178 212	42 70 101 134 178 212
	7	**26.2010**	26.1865	26.1843	26.184	26.1853	26.1843	38 67 100 133 174 197 221	37 64 97 133 174 198 221	37 65 99 133 174 197 223	38 67 98 133 174 197 223	37 65 99 134 174 198 223	37 65 99 133 174 197 223
STARFISH	5	**21.5771**	21.5733	21.5748	21.576	21.575	21.5748	48 89 129 168 207	46 86 127 168 208	49 88 128 167 206	49 90 130 168 206	46 86 127 168 207	49 88 128 167 206
	6	**24.1855**	24.1833	24.1847	24.1847	24.1838	24.1833	41 74 108 142 177 212	41 75 109 144 180 214	41 75 108 143 177 212	41 75 108 143 177 212	41 74 110 144 178 213	41 75 109 144 180 214
	7	**26.6605**	26.6596	26.6581	26.6592	26.6581	26.6581	37 67 97 127 157 186 217	38 68 98 128 158 163 218	37 67 97 131 159 189 219	37 67 98 129 159 189 218	37 67 97 131 159 189 219	37 67 97 131 159 189 219
FISHING	5	**20.0889**	20.0875	20.0877	20.0875	20.0877	20.0877	44 93 140 182 233	46 94 140 183 233	44 93 140 183 233	46 94 140 183 233	44 93 140 183 233	44 93 140 183 233
	6	**22.8738**	22.8722	22.8735	22.8722	22.8735	22.8735	42 83 126 167 202 237	42 82 125 166 201 237	41 82 125 167 202 237	42 82 125 166 201 237	41 82 125 167 202 237	41 82 125 167 202 237
	7	**25.5330**	25.5246	25.5258	25.5262	25.5270	25.5246	36 67 103 138 169 203 237	35 68 104 137 170 203 237	36 68 102 139 170 202 237	35 66 100 136 168 201 237	36 67 102 138 170 207 239	35 68 104 137 170 203 237
LENA	5	**20.1768**	20.1768	20.1768	20.1768	20.1768	20.1768	108 139 169 199 227	108 139 169 199 227	108 139 169 199 227	108 139 169 199 227	108 139 169 199 227	108 139 169 199 227
	6	**22.5014**	22.5006	22.5001	22.5005	22.5006	22.5001	83 109 138 169 198 227	83 110 141 169 200 228	83 111 141 171 199 228	83 109 141 170 199 227	83 110 141 169 200 228	83 111 141 171 199 228
	7	**24.7415**	24.7408	24.7394	24.7379	24.7408	24.7408	83 108 134 159 181 205 228	83 107 130 153 178 204 228	82 106 128 150 174 201 228	81 107 132 154 178 202 229	83 107 130 153 178 204 228	83 107 130 153 178 204 228
MAN	5	**20.8670**	20.8654	20.8654	20.8654	20.8654	20.8654	57 90 137 181 214	58 93 138 181 214	58 93 138 181 214	58 93 138 181 214	58 93 138 181 214	58 93 138 181 214
	6	**23.4229**	23.4219	23.4189	23.4219	23.4165	23.4165	57 90 133 162 192 219	57 90 134 162 192 218	58 91 134 164 192 219	57 90 134 162 192 218	58 90 133 165 192 219	58 90 133 165 192 219
	7	**25.8582**	25.8508	25.8464	25.8405	25.8464	25.8405	55 86 110 136 164 191 219	56 86 112 136 166 192 219	53 84 109 135 166 192 216	58 87 112 137 167 192 220	53 84 109 135 166 192 216	58 87 112 137 167 192 220
PEPPERS	5	20.9682	20.9676	20.9676	20.9676	20.9682	20.9682	44 75 104 143 180	44 75 104 143 181	44 75 104 143 181	44 75 104 143 181	44 75 104 143 180	44 75 104 143 180
	6	**23.4602**	23.4588	23.4596	23.4588	23.4596	23.4588	43 72 101 131 159 188	41 71 100 129 158 188	43 73 101 130 159 189	41 71 100 129 158 188	43 73 101 130 159 189	41 71 100 129 158 188
	7	**25.7929**	25.7835	25.7808	25.7808	25.7835	25.7835	27 54 81 104 131 161 191	27 55 81 106 135 160 191	28 55 83 107 135 160 190	28 55 83 107 135 160 190	27 55 81 106 135 160 191	27 55 81 106 135 160 191

Bold signifies the best result obtained by the proposed algorithm

Fig. 4 5, 6, and 7-level segmented starfish images by the IEHO, CEHO, OEHO, EHO and, AHA algorithms

where Ω represents the spacial domain of entire image and $S_L(X) = S_{pC}(X)S_G(X)$. $S_{pC}(X)$ and $S_G(X)$ are given by:

$$S_{pC}(X) = \frac{2PC_1(X)PC_2(X) + T_1}{PC_1^2(x) + PC_2^2 + T_1} \text{ and } S_G(X) = \frac{2G_1(X)G_2(X) + T_2}{G_1^2(X) + G_2^(X) + T_2} \tag{26}$$

where PC_1 and PC_2 are the phase congruence maps taken out from two images $f_1(X)$, and $f_2(X)$, respectively; T_1 and T_2 are constants which are taken as $T_1 = 0.85$ and $T_2 = 160$, respectively. Higher value of FSIM indicates better segmentation.

Calculated PSNR, SSIM, and FSIM values of the segmented images in reference to the original images are shown Table 8. The result demonstrates that the quality of

Table 6 Fitness value along with the threshold values of different algorithms for green band of using Otsu's methods as objective function

Image	K	IEHO	CEHO	OEHO	EHO	ABC	AHA	IEHO	CEHO	OEHO	EHO	ABC	AHA
BOAT	5	**1289.5208**	1289.5049	1289.499	1289.4598	1289.499	1289.499	75 101 125 149 168	75 101 124 149 168	75 101 125 150 169	75 100 125 149 168	75 101 125 150 169	75 101 125 150 169
	6	**1296.5441**	1296.5136	1296.5136	1296.2568	1296.5136	1296.2568	75 100 122 144 161 172	53 79 107 135 165 217	74 100 121 143 161 172	74 97 119 143 161 173	74 100 121 143 161 172	74 97 119 143 161 173
	7	**1302.2128**	1302.1271	1301.9817	1302.106	1301.6917	1301.9817	71 92 109 127 146 162 173	69 92 109 128 147 162 173	68 90 106 124 145 161 173	70 90 106 125 145 161 172	69 91 107 127 146 161 174	68 90 106 124 145 161 173
STARFISH	5	**3025.2944**	3025.2882	3025.2195	3025.2944	3025.2195	3025.2944	57 93 128 161 201	57 93 128 162 201	57 94 129 162 202	57 93 128 161 201	57 94 129 162 202	57 93 128 161 201
	6	**3054.6467**	3054.6342	3054.6467	3054.6336	3054.6467	3054.6467	53 84 113 141 170 206	53 85 114 142 171 206	53 84 113 141 170 206	52 84 113 141 170 206	53 84 113 141 170 206	53 84 113 141 170 206
	7	**3073.7606**	3073.7541	3073.5228	3073.5228	3073.6915	3073.5228	49 76 102 127 152 178 210	49 76 102 128 153 179 211	48 77 103 127 152 179 212	48 77 103 127 152 179 212	49 77 103 128 154 180 212	48 77 103 127 152 179 212
FISHING	5	**5032.6412**	5032.6366	5032.625	5032.6244	5032.6244	5032.6244	69 102 130 162 217	69 102 130 162 218	69 102 131 163 217	69 103 131 163 218	69 103 131 163 218	69 103 131 163 218
	6	**5052.9553**	5052.9452	5052.9346	5052.9393	5052.9346	5052.9346	59 88 112 138 168 220	58 88 112 137 167 219	58 87 112 138 168 220	58 88 112 138 168 220	58 87 112 138 168 220	58 87 112 138 168 220
	7	**5067.5081**	5067.465	5067.4546	5067.4463	5067.4463	5067.4546	53 81 104 126 149 176 223	51 80 103 126 149 177 223	52 80 103 126 150 178 224	52 81 104 127 151 179 225	52 81 104 127 151 179 225	52 80 103 126 150 178 224
LENA	5	2709.7936	2709.7936	2709.7936	2709.7936	2709.7936	2709.7936	46 80 110 139 174	46 80 110 139 174	46 80 110 139 174	46 80 110 139 174	46 80 110 139 174	46 80 110 139 174
	6	**2728.7969**	2728.7211	2728.683	2728.6830	2728.6877	2728.6830	42 73 99 122 148 179	41 69 94 118 145 177	42 73 96 121 147 179	42 73 96 121 147 179	43 72 96 121 147 180	42 73 96 121 147 179
	7	**2744.3351**	2744.1253	2744.3018	2744.0743	2744.3018	2744.3018	35 59 82 106 127 152 182	35 59 83 107 129 154 182	35 59 83 105 127 152 181	36 58 83 106 128 150 179	35 59 83 105 127 152 181	35 59 83 105 127 152 181
MAN	5	1800.7206	1800.7206	1800.7206	1800.7206	1800.7206	1800.7206	87 143 173 196 214	87 143 173 196 214	87 143 173 196 214	87 143 173 196 214	87 143 173 196 214	87 143 173 196 214
	6	**1813.7387**	1813.6832	1813.4844	1813.5692	1813.4844	1813.4844	83 135 160 182 200 215	84 136 162 183 199 215	83 136 163 183 200 216	85 135 161 182 199 216	83 136 163 183 200 216	83 136 163 183 200 216
	7	**1820.1302**	1820.0998	1819.9944	1819.9944	1820.0998	1820.0998	85 137 161 180 195 207 219	85 136 162 182 197 209 220	83 136 162 182 197 209 221	83 136 162 182 197 209 221	85 136 162 182 197 209 220	85 136 162 182 197 209 220
PEPPERS	5	5525.4596	5525.4596	5525.4596	5525.4596	5525.4596	5525.4596	29 71 116 159 192	29 71 116 159 192	29 71 116 159 192	29 71 116 159 192	29 71 116 159 192	29 71 116 159 192
	6	**5550.4761**	5550.4233	5550.3646	5550.3737	5550.3646	5550.3737	23 50 85 128 165 194	27 61 99 139 170 197	28 64 102 142 173 198	21 48 81 125 165 195	28 64 102 142 173 198	21 48 81 125 165 195
	7	**5571.4932**	5571.4812	5571.2964	5571.2964	5571.4589	5571.2964	20 44 72 110 146 175 198	19 44 74 110 146 173 198	21 45 73 111 144 174 197	21 45 73 111 144 174 197	20 45 73 107 144 173 198	21 45 73 111 144 174 197

Bold signifies the best result obtained by the proposed algorithm

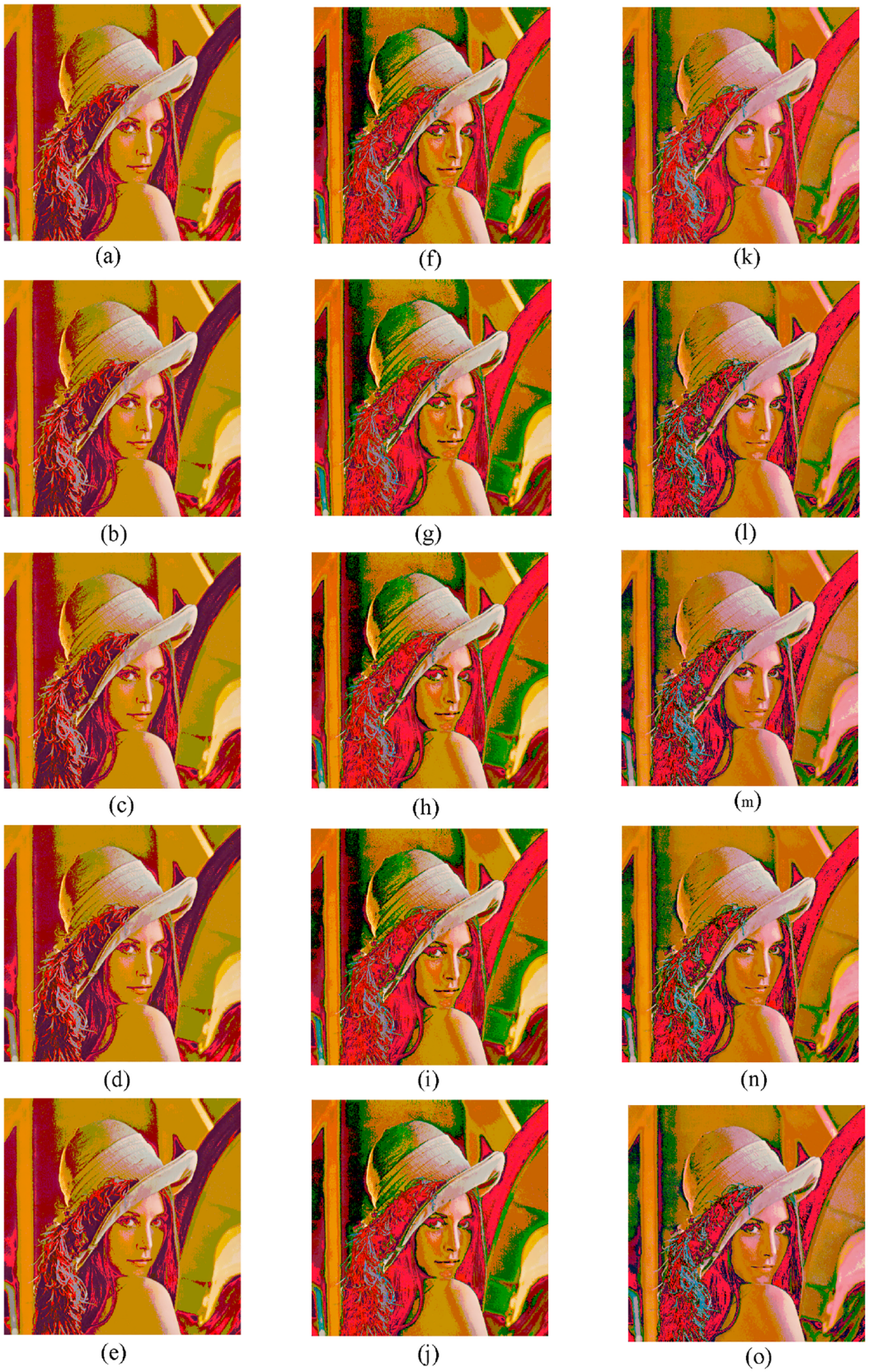

Fig. 5 5,6, and 7-level segmented lena images by the IEHO, CEHO, OEHO, EHO and ABC algorithms

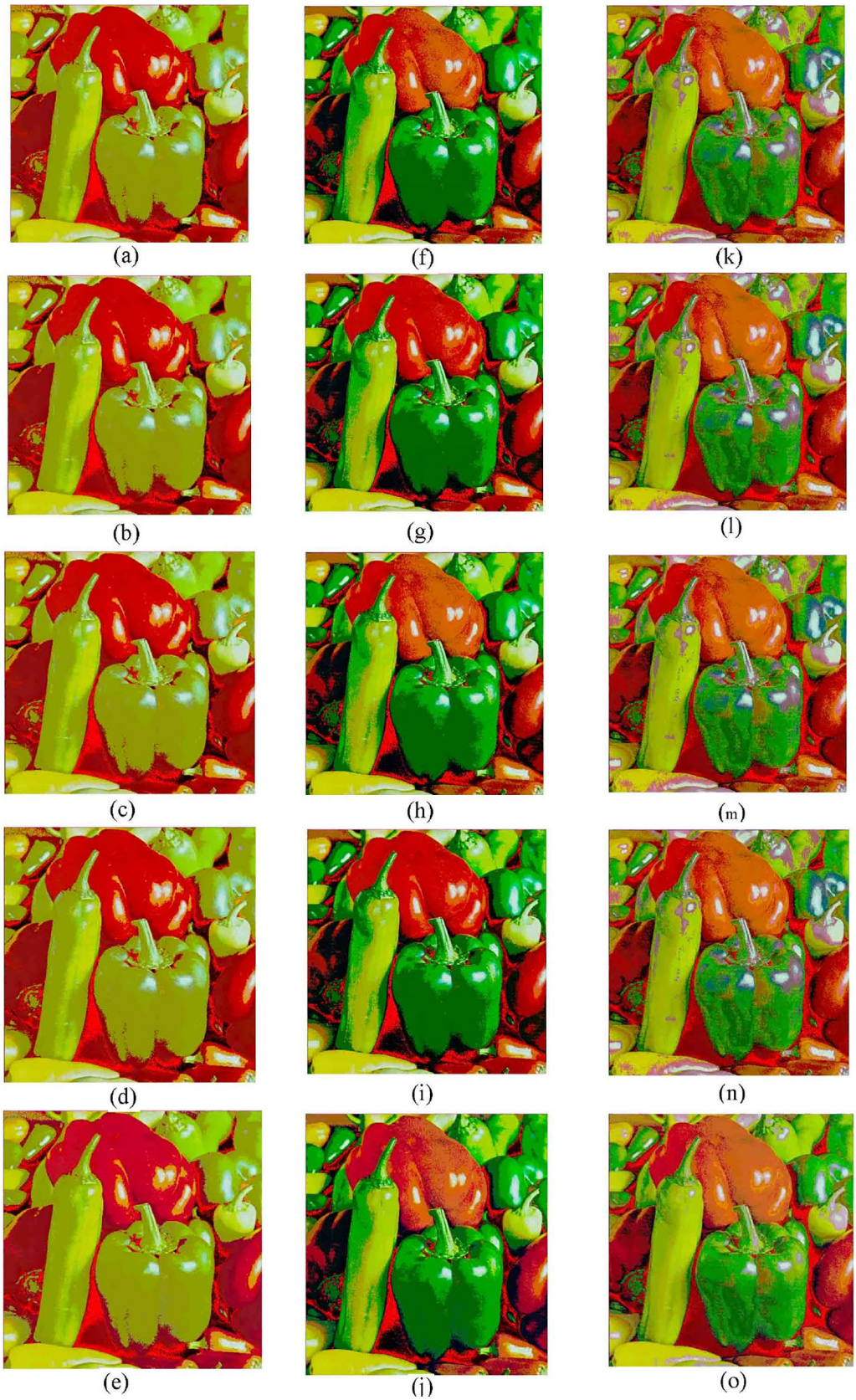

Fig. 6 5,6, and 7-level segmented Peppers images by the IEHO, CEHO, OEHO, EHO and ABC algorithms

Table 7 Fitness value along with the threshold values of different algorithms for blue band of using Masi's method as objective function

Image	K	IEHO	CEHO	OEHO	EHO	ABC	AHA	IEHO	CEHO	OEHO	EHO	ABC	AHA
BOAT	5	**15.5078**	15.5067	15.5050	15.5050	15.5067	15.5050	78 106 135 170 212	78 105 134 170 212	78 106 134 170 211	78 106 134 170 211	78 105 134 170 212	78 106 134 170 211
	6	**17.5436**	17.5334	17.5262	17.5334	17.5262	17.5262	78 107 137 170 210 229	76 106 135 170 210 231	76 106 137 171 209 231	76 106 135 170 210 231	76 106 137 171 209 231	76 106 137 171 209 231
	7	**19.4827**	19.4663	19.4663	19.4791	19.4791	19.4791	76 104 127 154 180 210 229	70 95 123 151 179 210 231	70 95 123 151 179 210 231	73 100 127 153 180 210 231	73 100 127 153 180 210 231	73 100 127 153 180 210 231
STARFISH	5	**15.9223**	15.9219	15.9219	15.9219	15.9219	15.9219	56 94 133 172 208	56 94 132 172 208	56 94 132 172 208	56 94 132 172 208	56 94 132 172 208	56 94 132 172 208
	6	**18.0202**	18.0199	18.0199	18.0186	18.0186	18.0186	48 77 110 144 177 208	51 82 115 146 180 208	51 82 115 146 180 208	49 79 111 142 177 208	49 79 111 142 177 208	49 79 111 142 177 208
	7	**20.0456**	20.0413	20.0362	20.0343	20.0362	20.0343	34 61 91 121 150 181 208	34 60 91 120 150 183 208	31 57 87 118 146 177 208	33 59 89 120 155 183 208	31 57 87 118 146 177 208	33 59 89 120 155 183 208
FISHING	5	**15.0782**	15.0781	15.0781	15.0781	15.0781	15.0781	51 99 148 190 236	52 100 148 190 236	52 100 148 190 236	52 100 148 190 236	52 100 148 190 236	52 100 148 190 236
	6	**17.3112**	17.3102	17.3096	17.3096	17.3102	17.3102	39 75 113 152 190 236	39 78 115 153 190 236	39 75 115 152 190 236	39 75 115 152 190 236	39 78 115 153 190 236	39 78 115 153 190 236
	7	**19.3864**	19.3799	19.3791	19.3775	19.3799	19.3799	36 65 96 128 157 189 236	33 66 93 124 157 190 236	37 69 98 131 158 190 236	37 67 99 128 157 192 236	33 66 93 124 157 190 236	33 66 93 124 157 190 236
LENA	5	**15.0032**	15.0025	15.0017	15.0025	15.0017	15.0017	79 107 135 165 195	80 108 135 165 195	79 106 134 166 195	80 108 135 165 195	79 106 134 166 195	79 106 134 166 195
	6	**16.8947**	16.8931	16.8908	16.8908	16.8931	16.8931	79 104 131 154 177 200	78 103 132 154 177 200	81 105 132 155 177 200	81 105 132 155 177 200	78 103 132 154 177 200	78 103 132 154 177 200
	7	**18.7161**	18.6900	18.7095	18.6900	18.7095	18.7095	73 93 112 134 156 178 200	70 91 115 135 154 179 200	75 95 115 135 155 177 200	70 91 115 135 154 179 200	75 95 115 135 155 177 200	75 95 115 135 155 177 200
MAN	5	**15.8488**	15.8472	15.8472	15.8472	15.8472	15.8472	51 87 128 163 198	52 87 127 162 198	52 87 127 162 198	52 87 127 162 198	52 87 127 162 198	52 87 127 162 198
	6	**17.8849**	17.8837	17.8837	17.8791	17.8791	17.8791	27 55 88 128 163 198	27 54 87 129 164 198	27 54 87 129 164 198	27 52 87 128 163 198	27 52 87 128 163 198	27 52 87 128 163 198
	7	**19.8540**	19.8366	19.8432	19.8432	19.8366	19.8366	28 54 87 112 137 166 198	27 53 83 108 133 166 198	26 53 87 116 141 166 199	26 53 87 116 141 166 199	27 53 83 108 133 166 198	27 53 83 108 133 166 198
PEPPERS	5	**15.9582**	15.9559	15.9559	15.9554	15.9554	15.9554	50 90 121 154 188	50 90 121 155 187	50 90 121 155 187	50 90 122 159 191	50 90 122 159 191	50 90 122 159 191
	6	**18.0274**	18.0255	18.0250	18.0244	18.0255	18.0255	47 75 104 132 165 196	46 74 104 135 166 196	47 76 106 136 167 197	47 74 105 135 166 197	46 74 104 135 166 196	46 74 104 135 166 196
	7	**19.9900**	19.9810	19.9821	19.9821	19.9810	19.9821	46 74 101 125 150 177 201	46 72 101 125 147 173 201	44 69 98 124 151 178 202	44 69 98 124 151 178 202	46 72 101 125 147 173 201	44 69 98 124 151 178 202

Bold signifies the best result obtained by the proposed algorithm

Table 8 PSNR, FSIM, SSIM of segmented images

		PSNR (dB)						SSIM						FSIM					
Image	K	IEHO	CEHO	OEHO	EHO	ABC	AHA	IEHO	CEHO	OEHO	EHO	ABC	AHA	IEHO	CEHO	OEHO	EHO	ABC	AHA
BOAT	5	**30.6872**	30.6328	30.6046	30.6003	30.6046	30.6332	**0.9518**	0.9511	0.9496	0.9517	0.9496	0.9494	**0.9630**	0.9618	0.9615	0.9613	0.9613	0.9615
	6	**32.1330**	32.1148	31.9702	31.9626	31.9598	31.9985	**0.9220**	0.9218	0.9200	0.9181	0.9120	0.9125	**0.9588**	0.9584	0.9544	0.9600	0.9552	0.9568
	7	**34.2639**	34.2022	33.9154	33.7924	33.8722	33.7484	**0.9479**	0.9465	0.9387	0.9395	0.9360	9384	**0.9043**	0.9023	0.9006	0.9021	0.9027	0.9028
STARFISH	5	**31.4494**	31.4347	31.4118	31.3848	31.3920	31.2145	**0.9545**	0.9545	0.9531	0.9524	0.9520	0.9531	**0.9423**	0.9422	0.9412	0.9408	0.9397	0.9398
	6	**33.8848**	33.8255	33.707	33.6204	33.6438	33.7458	**0.9070**	0.9070	0.9018	0.9063	0.9057	0.9045	**0.9179**	0.9166	0.9159	0.9160	0.9117	0.9156
	7	**35.4377**	35.4288	35.422	35.4227	34.3971	34.3885	**0.9098**	0.9097	0.9097	0.9083	0.9088	0.9086	**0.9352**	0.9300	0.9282	0.9296	0.9295	0.9299
FISHING	5	**33.3233**	33.2988	33.2982	33.2621	33.2349	33.2546	0.9778	0.9778	0.9775	0.9773	0.9772	0.9770	**0.9563**	0.9553	0.9563	0.9541	0.9533	0.9533
	6	**35.9833**	35.9145	35.9128	34.9006	34.8252	34.7895	**0.9595**	0.9589	0.9581	0.9584	0.9576	0.9578	**0.9524**	0.9520	0.9509	0.9502	0.9470	0.9502
	7	**37.5121**	37.445	37.3384	37.3245	37.3054	37.3658	**0.9720**	0.9701	0.9692	0.9694	0.9702	0.9695	**0.9862**	0.9829	0.9711	0.9720	0.9708	0.9715
LENA	5	**31.2315**	31.2309	31.2309	31.2315	31.2315	31.2315	**0.9482**	0.9480	0.9480	0.9482	0.9482	0.9482	0.9192	0.9192	0.9192	0.9192	0.9192	0.9192
	6	**33.8542**	33.8169	33.764	33.7348	33.7456	33.7589	**0.9066**	0.9047	.9031	0.9030	0.9041	0.9040	**0.9360**	0.9302	0.9311	0.9277	0.9298	0.9298
	7	**35.137**	35.0815	35.0149	34.8153	34.7766	34.7854	**0.9568**	0.9238	0.9214	0.9239	0.9193	0.9215	**0.9048**	0.9770	0.9983	0.9656	0.9925	0.9936
MAN	5	**32.7915**	32.7844	32.7092	3.7092	32.7092	32.7589	**0.9934**	0.9899	0.9905	0.9905	0.9905	0.9905	**0.9523**	0.9475	0.9477	0.9477	0.9477	0.9477
	6	**34.0061**	33.844	33.9985	33.8712	33.827	33.8541	**0.9287**	0.9217	0.9282	0.9217	0.9224	0.9215	**0.9604**	0.9600	0.9517	0.9473	0.9489	0.9487
	7	**36.4000**	36.3615	36.1345	36.3271	36.3904	36.2546	**0.9876**	0.9860	0.9840	0.9852	0.9844	0.9845	**0.9484**	0.9473	0.9473	0.9338	0.9466	0.9471
PEPPERS	5	**31.2744**	31.2669	31.2669	31.2669	31.2615	31.2668	**0.9504**	0.9489	0.9489	0.9489	0.9501	0.9501	**0.9556**	0.9555	0.9555	0.9555	0.9548	0.9551
	6	**33.2739**	33.2699	32.8334	33.0082	32.8606	32.8687	**0.9158**	0.9074	0.9139	0.9067	0.9137	0.9084	**0.9146**	0.9107	0.9976	0.9924	0.9936	0.9939
	7	**35.5331**	35.4016	35.4488	35.4488	35.4201	35.4857	**0.9201**	0.9175	0.9183	0.9183	0.9175	0.9175	**0.9205**	0.9205	0.9116	0.9134	0.9129	0.9188

Bold signifies the best result obtained by the proposed algorithm

Table 9 Mean and SD of blue band color space using Otsu's method as objective function

Image	K	MEAN						SD					
		IEHO	CEHO	OEHO	EHO	ABC	AHA	OCEHO	CEHO	OEHO	EHO	ABC	AHA
BOAT	5	**2090.1911**	2090.1772	2090.1680	2090.1701	2090.1664	2090.1785	**0.001329406**	0.009955589	0.009533362	0.004664233	0.010257602	0.01125668
	6	**2098.7958**	2098.3074	2098.6781	2098.4447	2098.3228	2098.4587	**0.528911046**	1.040892558	0.658500847	1.034196514	1.053669061	0457889615
	7	**2105.3711**	2105.2583	2105.1871	2104.8951	2105.0633	2105.2546	**1.006107584**	1.085301107	1.061987781	1.13646479	1.073491125	0.00254788
STARFISH	5	**1597.6178**	1597.5114	1597.5124	1597.5416	1597.5482	1597.5235	**0.037518211**	0.038817553	0.040337586	0.263554546	0.246414323	0.21456854
	6	**1610.3598**	1610.3129	1610.2271	1607.1396	1607.0203	1607.2145	**0.249978855**	0.332897957	0.401735109	0.528884085	0.689965169	0.61254788
	7	**1618.5820**	1618.1460	1617.4794	1616.8524	1617.14608	1617.3545	**0.540595550**	0.845127688	1.564837589	1.384849571	1.540972414	1.56214566
FISHING	5	**7422.9517**	7422.9287	7422.9138	7422.9115	7422.9103	7422.9145	**0.000494975**	0.031658051	0.036472064	0.028323023	0.003744496	0.00256545
	6	**7445.0819**	7444.9592	7444.8111	7444.0367	7444.4636	7444.7758	**0.829848938**	0.873944215	0.915572188	1.867978035	1.393666415	1.81456988
	7	**7461.9356**	7460.6320	7459.6270	7460.3899	7460.1069	7460.2514	**1.27874144**	2.389208835	2.705424629	2.393019989	2.411376469	2.35847899
LENA	5	**1116.9212**	1116.8893	1116.9001	1116.8413	1116.8412	1116.7458	**0.014393858**	0.122319456	0.02408622	0.18516369	0.183354361	0.18547896
	6	**1126.8347**	1126.7092	1126.2164	1126.5261	1126.3677	1126.4587	**0.540150117**	0.659919549	1.025924571	0.886859204	0.978866197	0.87456985
	7	**1134.1903**	1133.4973	1133.0444	1133.8550	1133.7486	1133.7458	**0.03687895**	0.192775684	0.424189294	0.66555057	0.682528197	0.54789665
MAN	5	**1228.0819**	1228.0708	1228.0605	1228.0600	1228.0626	1228.0611	**0.005060243**	0.005879471	0.005789724	0.035709853	0.041297336	0.06541256
	6	**1236.7477**	1236.6224	1236.4268	1235.9010	1236.0839	1236.085	**1.029919676**	1.034483597	1.161163631	1.472726905	1.502514046	1.56521145
	7	**1243.2288**	1243.1099	1242.7293	1242.8587	1242.9911	1242.8854	**0.57895511**	0.656947726	0.777203984	0.705564838	0.752688662	0.71258693
PEPPERS	5	**1881.3815**	1881.3812	1881.3808	1881.3803	1881.3700	1881.3002	**0.014775883**	0.014788798	0.01465899	0.014513599	0.036593482	0.02544788
	6	**1902.2516**	1902.2043	1902.1466	1901.1904	1901.7507	1901.8789	**0.404328324**	0.437603459	0.479491887	1.343849532	1.649688597	1.56874582
	7	**1913.1695**	1913.1064	1912.9847	1912.8316	1912.9378	1912.8857	**0.454452365**	0.471188621	0.472820477	0.554560964	0.486465856	0.45896552

Bold signifies the best result obtained by the proposed algorithm

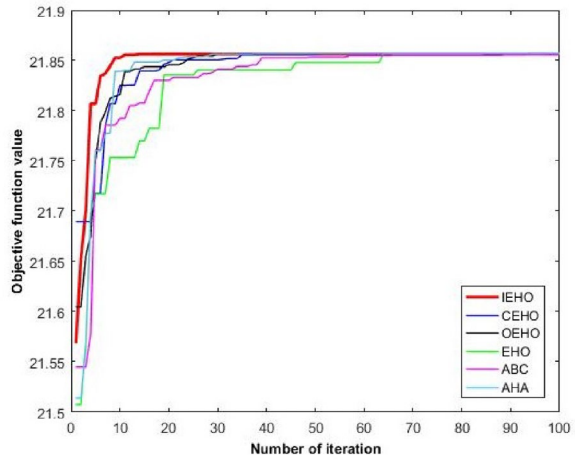

(a) 5-level thresholding of green band of Starfish image using Kapur methods

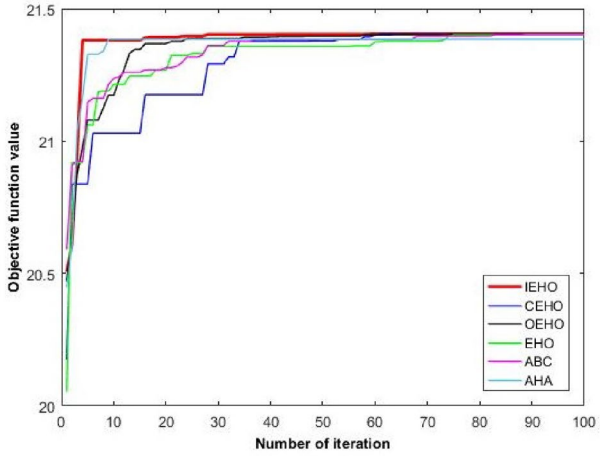

(b) 5-level threshold of green band of man image using Kapur methods

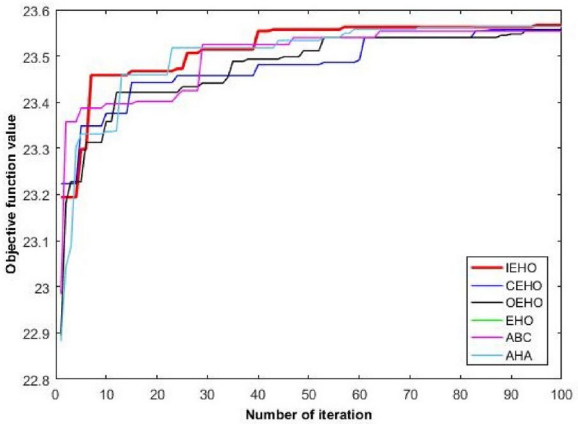

(c) 6-level threshold of blue band Starfish image using Kapur methods

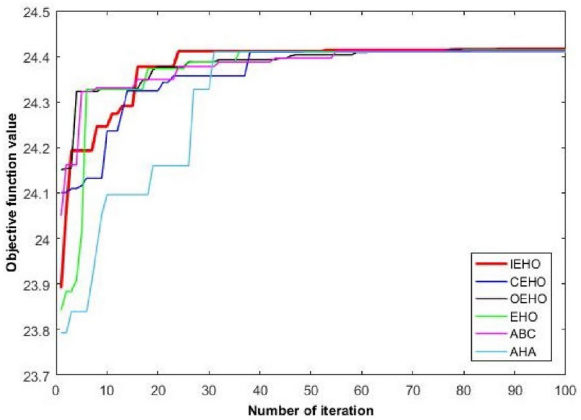

(d) 6-level threshold of red band of man image using Kapur methods

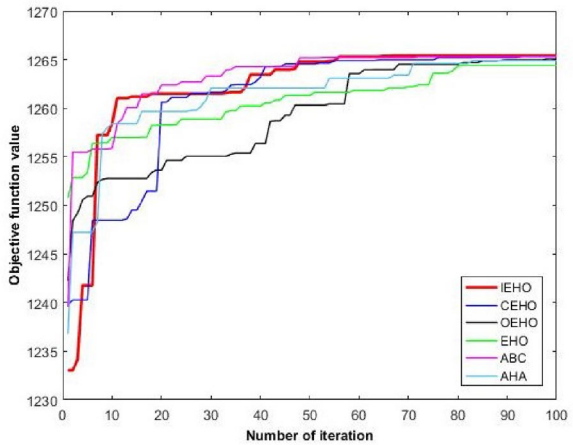

(e) 7-level thresholding of blue band of Starfish image using Otsu methods

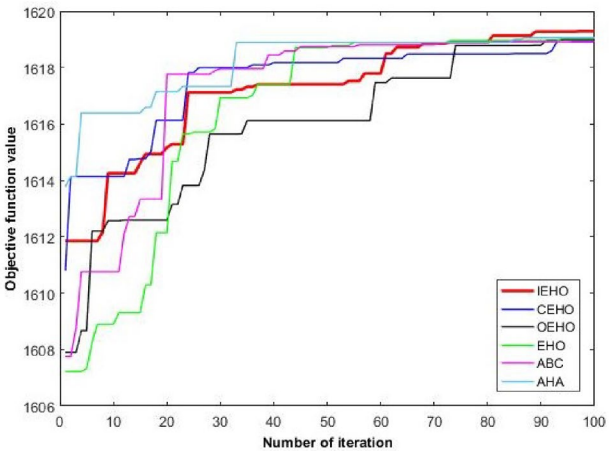

(f) 7-level thresholding of red band of man image using Otsu methods

Fig. 7 5-6-7 level convergence graph of starfish and man images using Kapur's and Otsu's objective functions

the segmented images is improved after integrating both the chaotic and oppositional ideas into the EHO instead of separately integrating the chaotic and oppositional with the EHO. It is also shown that the proposed algorithm is more suitable for a higher level of segmentation, which represents higher instability.

5.2 Stability

Due to the pseudo-random nature of the meta-heuristic search, we cannot make a concrete decision on an algorithm's performance by executing it only once. Therefore, an algorithm should be repeatedly executed to decide the performance of the algorithm. The optimal results are obtained by computing the mean and standard deviation. The process is useful to determine the stability of the algorithm. Higher mean values imply better performance in segmentation, and the lower standard deviation values indicate the algorithm's stability factor. Hence, the present authors have executed each algorithm 30 times and recorded the mean and standard deviation of the metrics. Table 9 shows the recorded values of an Otsu method for the selected images. The results reveal that the performance of IEHO comes in the 1st position in terms of mean and SD values among all the other algorithms followed by OEHO, CEHO, EHO, and others. This indicates that the proposed IEHO has less tends to get stuck into local optima, producing a stable result every time.

5.3 Convergence property

The convergence characteristics curve (objective function value vs. the number of iteration) of different algorithms obtained for the 5, 6, and 7-level thresholding of different images are shown in Fig. 7. for different fitness functions. Figure 7(a) and (b) show the convergence rate for 5-level thresholding of starfish and man images using Kapur's and Otsu's objective functions in IEHO, OEHO, CEHO, EHO,ABC and AHA algorithms. Figure 7(c) and (d) show the algorithms' convergence behavior for the 6-level thresholding of the same set of images for all the algorithms. Figure 7(e) and (f) show the convergence plots for 7-level thresholding of the same images.The plots reveal that the IEHO appears to be most steady among all approaches by accomplishing the ideal fitness in fewer iterations. It demonstrates its capacity to maintain a strategic distance from the chances of premature convergence by getting away from being caught in local optima.

5.3.1 Statistical analysis

Wilcoxon rank-sum [38], a non-parametric statistical investigation test, has been conducted with a 5% significant level to test the critical contrast among the proposed algorithm with the other considered algorithms. The mean value of Otsu's objective function of the blue band is taken for comparing the performance of IEHO and the OEHO, CEHO, EHO, ABC, AHA. Table 4 shows the p-value and the h-value of Wilcoxon's test of the four groups namely, IEHO vs OEHO, IEHO vs. CEHO, IEHO vs. EHO, IEHO vs. ABC and IEHO vs. AHA. A null hypothesis $[(p > 0.05)$ and $(h = 0)]$ assumes that there is no critical contrast between mean values which is indicated by the '#' symbol, whereas '*' signifies the alternative hypothesis $[(p < 0.05)$ and $(h = 1)]$ reflects a critical distinction between the four algorithms. The results in Table 4 explore that, for most of the cases, the proposed IEHO provides better performance than the others discussed algorithms.

6 Conclusions and future research directions

Premature convergence is the main challenge of any nature-inspired meta-heuristic algorithm. Most evolutionary algorithms used the stochastic property to utilize the search space, comprehensively influencing premature convergence. This study proposed a novel IEHO to find the optimal thresholds in multilevel image thresholding by integrating the concepts of oppositional and chaos into the basic EHO algorithm to maintain a strategic distance from premature convergence and improve the performance of the essential EHO.The proposed algorithm has been compared with a different combination of oppositional and chaotic EHO algorithms. The performance is measured by optimizing three image segmentation techniques: Otsu, Kapur, and Masi's entropy-based objective function for standard test images to find the ideal thresholds in multilevel image segmentation. This study's qualitative and quantitative investigation exposes the proposed algorithm's efficiency over the other algorithms. Thus, using chaotic sequence and the oppositional concepts with the basic EHO is an excellent alternative to avoid local optimality by diversifying its searching ability, reducing the chances of premature convergence. Hence, the IEHO confirms a more stable and robust algorithm in multilevel image segmentation. Thus, the proposed algorithm can be effectively used in the medical domain to accurately identify the various objects in the medical images, which helps diagnose diseases properly.

In future, the proposed algorithm can be used to optimize other research domain problems. Moreover, the proposed

algorithm can be combined with the machine learning model and it can be applied to different real-time medical applications to predict or classify diseases of various categories. On the other hand, the proposed algorithm can also be used in feature selection and shape optimization problemss.

Author contributions All authors contributed to the study conception and design. Material preparation, data collection and analysis were performed by Dr. Falguni Chakraborty and Dr. Provas Kumar Roy. The first draft of the manuscript was written by Dr. Falguni Chakraborty and all authors commented on previous versions of the manuscript. All authors read and approved the final manuscript.

Funding The authors declare that no funds, grants, or other support were received during the preparation of this manuscript

Data availability statement The data that support the findings of this study are available on request from the corresponding author. The data are not publicly available due to restrictions e.g., their containing information that could compromise the privacy of research participants.

Declarations

Conflict of interest The authors declare that they have no known competing financial interests or personal relationships that could have appeared to influence the work reported in this paper.

Ethical approval This article does not contain any studies with human participants or animals performed by any of the authors.

References

1. Abdul Kayom Md, Khairuzzaman Saurabh Chaudhury (2017) Multilevel thresholding using grey wolf optimizer for image segmentation. Expert Syst Appl 86:64–76
2. Abdulhameed S, Rashid TA (2022) Child drawing development optimization algorithm based on child's cognitive development. Arab J Sci Eng 47:1337–1351
3. Akay B (2013) A study on particle swarm optimization and artificial bee colony algorithms for multilevel thresholding. Appl Soft Comput 13:3066–3091
4. Alatas B (2010) Chaotic harmony search algorithms. Appl Math Comp 216(9):2687–2699
5. Aziz Mohamed Abd El, Ewees Ahmed A (2017) Aboul Ella Hassanien. Whale optimization algorithm and Moth-Flame optimization for multilevel thresholding image segmentation. Expert Syst Appl 83:242–256
6. Bhandari AK, Kumar A, Chaudhary S, Singh GK (2016) A novel color image multilevel thresholding based segmentation using nature inspired optimization algorithms. Expert Syst Appl 63:112–133
7. Bhuyan S, Agrawal S, Panda R, Panigrahi BK (2013) Tsallis entropy based optimal multilevel thresholding using cuckoo search algorithm. Swarm Evolut Comp 11:16–30
8. Chnoor M, Rashid A (2021) A new evolutionary algorithm: learner performance based behavior algorithm. Egypt Info J 22(2):213–223
9. Gandomi A, Yang X (2014) Chaotic bat algorithm. J Comp Sci 5:224–232
10. Gandomi A, Yang X, Talatahari S, Alavi A (2013) Firefly algorithm with chaos. Commun Nonlinear Sci Numer Simul 18(1):89–98
11. Gandomi A, Yun G, Yang X, Talatahari S (2013) Chaos-enhanced accelerated particle swarm algorithm. Commun Nonlinear Sci Numer Simul 18(2):327–340
12. Gupta Rohan, Sharma Anjali, Singh Vikram (2024) Enhanced whale optimization algorithm for lung CT image segmentation in lung cancer diagnosis. IEEE Access 11547–11558
13. Hama Rashid DN, Rashid TA, Mirjalili S (2021) ANA: ant nesting algorithm for optimizing real-world problems. Mathematics 9(23):3111
14. He Lifang, Huang Songwei (2017) Modified firefly algorithm based multilevel thresholding for color image segmentation. Neurocomputing 240:152–174
15. Horng MH (2010) Multilevel minimum cross entropy threshold selection based on the honeybee mating optimization. Expert Syst Appl 37:4580–4592
16. Jin H, Tao W, Liu L (2007) Object segmentation using ant colony optimization algorithm and fuzzy entropy. Pattern Recogn Lett 28(7):788–796
17. Kapur JN, Sahoo PK, Wong AKC (1985) A new method for gray-level picture thresholding using the entropy of the histogram. Comp Vision Gr Image Process 29:273–285
18. Kim Hyun, Lee Min-Soo, Park Ji-Hoon (2023) Firefly algorithm for segmentation of retinal images to detect diabetic retinopathy, 210:106365
19. Lin Z, Lei Z, Xuanqin M, Zhang D (2011) FSIM: a feature similarity index for image quality assessment. IEEE Trans Image Process 20(8):2378–2386
20. MSaleh Tavazoei, Haeri M (2007) Comparison of different one-dimensional maps as chaotic search pattern in chaos optimization algorithms. Appl Math Comp 187:1076–1085
21. Mohammed HM, Rashid TA (2021) Chaotic fitness-dependent optimizer for planning and engineering design. Soft Comput 25:14281–14295
22. Otsu N (1979) A threshold selection method from gray-level histograms'. IEEE Trans SMC 9(1):62–66
23. Pare S, Bhandari AK, Kumar A, Singh GK (2018) A new technique for multilevel color image thresholding based on modified fuzzy entropy and Lévy flight firefly algorithm. Comp Electr Eng 70:476–495
24. Salama MMA, Rahnamayan S, Tizhoosh Hamid R (2008) Opposition-based differential evolution. IEEE Trans Evolut Comp 12(1):64–79
25. dos Santos Coelho L, Sauer JG, Rudek M (2009) Differential evolution optimization combined with chaotic sequences for image contrast enhancement. Chaos, Solitons Fractals 42(1):522–529
26. Sathya PD, Kayalvizhi R (2010) Optimum multilevel image thresholding based on tsallis entropy method with bacterial foraging algorithm. Int J Comp Sci 7(5):336–343
27. Sharma Priya, Verma Rahul (2022) Hybrid GA-PSO for multilevel segmentation of brain MRI images for tumor diagnosis. Med Image Anal 45:25–36
28. Shilpa S, Shyam L (2016) Multilevel tresholding based on Chaotic Darwinian particle swarm optimization for segmentation of satellite images. Appl Soft Comp 55:503–522
29. Shubham S, Bhandari AK (2019) A generalized Masi entropy based efficient multilevel thresholding method for color image segmentation. Multimed Tools Appl 78:17197–17238
30. Simon D (2008) Biogeography based optimization. IEEE Trans Evolut Comp 12(6):702–713
31. Singh A, Alam S, Guha D (2016) Optimal solutions of load frequency control problem using oppositional krill herd algorithm. IEEE First Int Conf Control, Measurement Instrum (CMI), pp 6–10

32. Talatahari S (2012) Gandomi AH, Yang XS, Deb S, Coupled eagle strategy and differential evolution for unconstrained and constrained global optimization. Comp Math Appl 63(1):191–200
33. Taleb-Ahmed A, Ouadfel S (2016) Social spiders optimization and flower pollination algorithm for multilevel image thresholding: a performance study. Expert Syst Appl 55:566–584
34. Tizhoosh HR (2005) Opposition-based learning: a new scheme for machine intelligence. Proc Int Conf Comput Intell Model Control Autom Vienna Austria 1:695–701
35. Tizhoosh HR, Rahnamayan S, Salama M (2008) Opposition versus randomness in softcomputing techniques. Appl Soft Comp 8(2):906–918
36. Wang GG, Deb S, Geo X-Z, Coelho LDS (2016) A new metaheuristic optimization algorithm motivated by elephant herding behavior. Int J Bio-Inspired Comp 8(6):394–409
37. Wang GG, Deb S, Gandomi AH, Zhang Z, Alavi AH (2016) Chaotic cuckoo search, Soft Comp, 1–14
38. Wilcoxon F (1945) Individual comparisons by ranking methods. Int Bio-Metric Soc 6:80–83
39. Wolpert DH, Macready WG (1997) No free lunch theorems for optimization. IEEE Trans Evol Comput 1:67–82
40. Wu XX, Chen Z (1996) Introduction of Chaos theory. Bibliographic Publishing House, Shanghai Science and Technology
41. Yang XS (2010) A new meta-heuristic bat-inspired algorithm. Stud Comp Intell 284:65–74
42. Yang XJ, Huang ZG (2012) Opposition-based artificial bee colony with dynamic cauchy mutation for function optimization. Int J Adv Comp Technol 4(4):56–62
43. Yin PY (1999) A fast scheme for multilevel thresholding using genetic algorithms. Signal Process 72:85–95
44. Yin PY (2007) Multilevel minimum cross entropy threshold selection based on particle swarm optimization algorithm. Appl Math Comp 184(2):503–513
45. Zhou W, Alan CB, Hamid SR, Eero SR, Eero SP (2004) Image quality assessment: from error visibility to structural similarity. IEEE Trans Image Process 13(4):600–612
46. wang Hui, Wu Zhijian, Rahnamayan Shahryar, Liu Yong, Ventresca Mario (2011) Enhancing particle swarm optimization using generalized opposition-based learning. Inform Sci 181(20):4699–4714